International Journal of Biological Macromolecules 371 (2026) 152914

Contents lists available at ScienceDirect

International Journal of Biological Macromolecules

journal homepage: www.elsevier.com/locate/ijbiomac

Chitosan or ε-polylysine-functionalized mucoadhesive liposomes for enhanced intracellular delivery of Isoniazid

Jacopo Forte [a,1], Tommaso Olimpieri [b,1], Noemi Poerio [b], Leonardo Severini [c], Maurizio Fraziano [b], Maria Grazia Ammendolia [d], Federica Rinaldi [e,*], Simona Sennato [c,f,**], Carlotta Marianecci [e], Federico Bordi [f,2], Maria Carafa [e,2]

[a] Department of Basic Biotechnological Sciences, Intensivological and Perioperative Clinics, Catholic University of Sacred Heart, Largo Francesco Vito 1, 00168, Rome, Italy
[b] Department of Biology, University of Rome "Tor Vergata", Via della Ricerca Scientifica, Rome, 00133, Italy
[c] Institute of Complex Systems (ISC) – National Research Council (CNR), "Sapienza" branch, Piazzale A. Moro 5, Rome, 00185, Italy
[d] National Center for Innovative Technologies in Public Health, Italian National Institute of Health, Viale Regina Elena 299, Rome, 00161, Italy
[e] Department of Drug Chemistry and Technology, Sapienza University of Rome, Piazzale A. Moro 5, Rome, 00185, Italy
[f] Department of Physics, Sapienza University of Rome, Piazzale A. Moro 5, Rome, 00185, Italy

ARTICLE INFO

Keywords:
Chitosan
ε-Poly-L-lysine
Polycation-decorated liposome
Isoniazid
Intracellular delivery
Antibacterial activity

ABSTRACT

Polymer decoration is a widely used method for surface modification of liposomes which is able to improve the stability of the vesicles, mechanical resistance to aerosolization, mucoadhesion and targeting capabilities. Chitosan, a biocompatible polysaccharide, is an excellent candidate for this purpose and it is largely employed for the development of liposomal formulation for pulmonary delivery. The cationic polymer ε-poly-L-lysine is widely used as a food preservative while its use as a stabilizer and mucoadhesive agent is less explored. Here we consider the use of Chitosan and ε-poly-L-lysine to improve the properties of anionic liposomes entrapping Isoniazid, an anti-tubercular drug, to obtain stable, mucoadhesive nanocarriers capable of delivering Isoniazid into cells, for potential nasal administration. By using the same procedure for both polymers, we obtained liposomes decorated with Chitosan and ε-poly-L-lysine with the optimal size range for potential nasal administration and pulmonary deposition, capable of ensuring the stability of the entrapped drug both after three months of storage and after nebulization. These polymer-decorated liposomes show safe and effective intracellular delivery of Isoniazid to BCG-lux-infected macrophages, reducing intracellular mycobacteria viability.

1. Introduction

Chitosan and ε-poly-L-lysine have gained significant attention as naturally derived polymers to be used as decorating agents for liposomes, due to their combination of biocompatibility and biodegradability. Their positive charges enable electrostatic interaction and modulation of vesicle surface properties such as mucoadhesion, thus improving the performance of nanocarriers in the lung environment [1,2].

Among the many available nanocarriers, liposomes have proven to be highly effective in delivering antibacterial drugs to treat pulmonary infections [3]. Their use is particularly noteworthy because they are easy to prepare, generally safe, and capable of regulating drug release. However, some critical issues such as premature drug leakage may restrict their applicability. Polymer decoration represents a viable strategy to overcome these challenges thanks to the possibility to

* Corresponding author.
** Correspondence to: S. Sennato, Institute of Complex Systems (ISC) – National Research Council (CNR), "Sapienza" branch, Piazzale A. Moro 5, Rome, 00185, Italy.
E-mail addresses: jacopo.forte@unicatt.it (J. Forte), tommaso.olimpieri.6@gmail.com (T. Olimpieri), noemi.poerio@uniroma2.it (N. Poerio), leonardoseverini@cnr.it (L. Severini), fraziano@bio.uniroma2.it (M. Fraziano), maria.ammendolia@iss.it (M.G. Ammendolia), federica.rinaldi@uniroma1.it (F. Rinaldi), simona.sennato@cnr.it (S. Sennato), carlotta.marianecci@uniroma1.it (C. Marianecci), federico.bordi@roma1.infn.it (F. Bordi), maria.carafa@uniroma1.it (M. Carafa).
[1] These authors contributed equally to this work.
[2] These authors shared seniorship.

https://doi.org/10.1016/j.ijbiomac.2026.152914
Received 16 February 2026; Received in revised form 26 May 2026; Accepted 4 June 2026
Available online 6 June 2026

modulate the surface properties of liposomes to improve stability, pharmacokinetics and adhesive properties toward a specific target [4,5]. Chitosan (Chit, hereinafter), a semi-rigid polysaccharide with limited flexibility, is prepared by deacetylating chitin. Chit's behavior in solution is influenced by factors such as molecular weight, deacetylation degree and pH [6,7]. Chit's outstanding physicochemical and biological properties, namely antibacterial activity, low toxicity, hemocompatibility and muco-adhesiveness, to name a few, make it a highly promising candidate for a wide range of applications, ranging from environmental to biomedical sciences [8–11]. Chit is able to adsorb on and decorate anionic liposomal surface, owing to its cationic character, mainly by electrostatic interactions. This results in a higher stability against aggregation, higher thermal or storage stability [12,13] and improved mechanical stress resistance to nebulization, by properly balancing their charge ratio, a key-aspect in the nose-to-lung delivery of Chit-decorated liposomes. It has to be remarked that Chit is probably the most well-known mucoadhesive agent, since it increases the penetration of macromolecules and nanoparticles through the nasal and intestinal barriers, as first described by Lehr et al.in 1992[14]. This effect is due to its ability to electrostatically bind with the glycosylated regions of mucin fibers, which are densely negatively charged [15]. Conventional nanocarriers are likely to be trapped by mucus via steric or adhesive forces and rapidly eliminated via mucociliary clearance, so they cannot distribute throughout the lung airways nor long-reside in the lung and/or reach the airway epithelium. Therefore, their poor permeability through the mucosa often reduces the effectiveness of therapies [16]. To overcome the short transit time, research efforts focus on improving nanocarrier association to mucus. Mucoadhesion slows the particle transit time through the specific tract of the body to the time scale of mucus renewal, thereby enhancing drug absorption.

The design of mucoadhesive drug delivery systems is currently the predominant approach to improve pulmonary delivery of therapeutics [17]. Surface modification with Chit has been shown to be able to promote liposome interaction with airway mucus and the modulation of barrier properties of the mucus itself [18].

Recently, we have shown that the naturally occurring ε-poly-L-lysine (ε-PLL) is able to improve the mucoadhesion of anionic liposomes composed by a mixture of hydrogenated soy phosphatidylcholine-phosphatidylglycerol (HSPC–DPPG). Importantly, this occurs without affecting their colloidal features and the entrapment efficiency of the hydrophobic anti-tubercular drug Rifampicin [19,20]. ε-PLL decorated liposomes have also proven to be able to deliver Rifampicin on macrophages infected by *Mycobacterium abscessus* and to exert a therapeutic effect [19]. These findings suggest the possible use of ε-PLL decorated liposomes as intracellular nanocarriers to improve antibiotic delivery in the lung. ε-PLL is a flexible, low molecular weight polypeptide with highly mobile chains, with water-soluble properties [2] and a broad-spectrum of antimicrobial activity [21–23], biodegradable, biocompatible and largely used as food preservatives [24]. Since the earlier studies, the observed antimicrobial activity has been attributed to the polycation nature of its α-amino group, which is positively charged at neutral pH, thus enabling electrostatic adsorption on the bacteria cell surface [25]. Contrary to α-poly-lysine [26], in ε-PLL the L-lysine residues are linked together by amide bonds between the carboxyl group and the ε-amino group of two consecutive amino acids. This peculiar structure hinders the hydrophobic interaction with lipid bilayers and their consequent destabilization. This has encouraged the use of ε-PLL for stabilization of liposomes [27], lipid-surfactant vesicles [28,29] and for guiding the assembly of insulin proteins in nanospheres for pulmonary delivery applications [30]. Improvement of therapeutic management of pulmonary diseases has been examined by improving drug administration using mucoadhesive Chit-decorated liposomes, while ε-PLL has been rarely explored in this context. In a recent paper, the use of ε-PLL and Chit as decorating agents for anionic liposomes loading the Rifampicin showed that both polymers can improve mucoadhesion without affecting liposome features and entrapment efficiency of this antitubercular drug [21]. Interestingly, ε-PLL-decorated liposomes proved to exert more effective antibacterial action on Mycobacterium-abscessus-infected macrophages, compared to Chit-decorated liposomes. ε-PLL may offer additional advantages compared to Chit due to its pH-independent cationic charge and well-defined molecular weight, which ensure more reproducible interactions under physiological conditions. These features make ε-PLL particularly suitable for liposome stabilization and pulmonary drug delivery and provided new motivation to explore this less-studied polypeptide as a tool to improve antibiotic delivery in the lung.

In the panorama of liposomal delivery for treating pulmonary infections, recent attention has been paid to Isoniazid (INH) [31], one of the first-line antibiotics used to treat *Mycobacterium tuberculosis* infections. Among all anti-tubercular agents, INH stands as a cornerstone, recognized for its potent bactericidal activity against actively replicating bacteria. However, its efficacy is constrained by many challenges and limitations of conventional treatments, such as low permeability, rapid clearance from the body and toxic effects associated with the prolonged use [32]. INH-encapsulated liposomes represent a promising advancement in TB treatment and may offer several potential benefits over conventional formulations [19,20]. As reported in a previous investigation, anionic HSPC-DPPG liposomal formulation is also able to entrap INH in the vesicle aqueous compartment with high efficiency [33]. In HSPC-DPPG formulations, the presence of a strong drug-lipid interaction increases INH entrapment due to drug adsorption, which occurs both on inner and outer surface of liposomes, favored by the dipolar nature of INH at physiological pH, which drives a dipole-dipole interaction with zwitterionic lipids. With the perspective of development of a combinatorial therapeutic strategy for delivering INH and Rifampicin for a pulmonary administration, alternative to the co-delivery strategies described up to now in recent works [19], we optimized the preparation of liposomes composed by HSPC-DPPG entrapping INH and the polymer decorating by Chit and ε-PLL. We have chosen a HSPC-DPPG mixture close to the equimolar since at this lipid composition, we have shown that the heterogeneity of the lipid layer is the highest, thus allowing the largest INH insertion in the bilayers and a larger value of the entrapment ratio for INH loaded liposomes [31]. The possible presence of the drug on the liposomal surface could interfere with the surface decoration of the polymer. To the best of our knowledge, no similar studies with this hydrophilic drug and polymers with well distinct structural and electrical properties are available. The aim of our work is to study in detail the chemical-physical properties of liposomes decorated with Chit or ε-PLL that trap INH.

To test the effectiveness of the intracellular delivery of INH by these novel polymer-decorated INH nanocarriers, we evaluate their antimicrobial activity in the context of *Mycobacterium bovis* infections, used as a surrogate model for the preliminary investigation on potential anti-*Mycobacterium tuberculosis* therapies [32].

2. Materials and methods

2.1. Materials

1,2-Dipalmitoyl-sn-glycero-3-phosphorylglycerolsodium salt (DPPG, molecular weight Mw = 745 g/mol) and hydrogenated phosphatidylcholine from soybean (HSPC, molecular weight Mw = 790 g/mol) were a kind gift from LIPOID GmbH (Lipoid GmbH, Ludwigshafen, Germany). Isoniazid (INH nominal purity >97%), diphenylhexatriene (DPH), mucin, Hepes salt [N-(2-hydroxyethyl) piperazine-N-(2ethanesulfonic acid)]. Low molecular weight chitosan (Chit) from shrimp shells (deacetylation ≥75%; CAS: 9012-76-4; Lot: STBG5431V; molecular weight: 2–4 × 10^4 Da) powder was purchased from Sigma-Aldrich (St. Louis, MO, USA). It is composed of randomly distributed β (1 → 4)-D-glucosamine (75%) and *N*-acetyl-D-glucosamine (25%) units. At physiological pH (~7.4), Chit (pKa ~6.5) exhibits a low degree of protonation (~11% of its amino groups, corresponding to ~8.4% charged units

overall due to 75% deacetylation). The viscosity (1% w/v in 1% acetic acid =20–300 cps) is theoretically consistent with molecular weight, according to the manufacturer's information. According to the supplier, chitosan was obtained with purity higher than 99% [34]. ε-Poly-L-lysine (ε-PLL) was a gift from JNC-Chisso (Yokohama, Japan). It is produced by a mutant of *Streptomyces albulus* NBRC14147 strain, is composed of 25 to 35 L-lysine residues (Mw ~ 4000) and the α-amino group is positively charged at neutral pH. Phosphotungstic acid (PTA) was purchased by Sigma-Aldrich. All other products and reagents, purchased by Sigma-Aldrich, were of analytical grade.

2.2. Preparation of liposomes and polycation-liposome complexes

Liposomes (Lipo) and INH-loaded liposomes (LipoINH) were prepared using the Thin Layer Evaporation (TLE) technique, also known as the "film formation technique", by considering approximately equimolar mixtures of HSPC and DPPG, as reported in detail in our previous work [19]. For the preparation of liposomes, as reported in Table 1, lipids were accurately weighed, placed in a round-bottom flask and solubilized using a chloroform/methanol mixture (3:1 v/v). The organic solvent was removed by rotary evaporation (Heidolph VV2000, Büchi-Italia SRL, Assago, Italy) for approximately 1 h at a rotation speed of 120 rpm at room temperature. Residual traces of solvent were subsequently eliminated using an oil pump (Edwards E2M5, Stockholm, Sweden).

The lipid film formed on the walls of the flask was hydrated with Hepes buffer (pH = 7.4, 0.01 M) for Lipo or INH solution for LipoINH and mechanical energy was applied using a high-energy vortex mixer for approximately 3 min to facilitate the detachment of the lipid film from the flask walls, yielding a multilamellar liposomal suspension [33].

In order to obtain a unilamellar suspension, samples were sonicated by tip (amplitude 20%, temperature 4 °C, 4 min, pulse on 0.8 and pulse off 0.6) using an ultrasonic sonicator (Vibracell - VCX 500, Sonics, Taunton, MA, USA), under an inert atmosphere with continuous nitrogen flow to prevent phospholipid degradation, such as hydrolysis and/or oxidation, and to degas the hydrating buffer solution.

To purify the sample and remove unincorporated components, the suspension was initially centrifuged using an MPW-260R centrifuge at 600 RPM and 22 °C for 20 min. The supernatant was then subjected to ultracentrifugation using an OPTIMA*MAX-XP (Beckman Coulter) at 30.000 RPM and 4 °C for 2 h and 30 min.

Chit solution was prepared by dissolving the powder in acetate buffer (0.2 M, pH 4.4) up to desired concentration, and it was stirred overnight.

ε-PLL was dissolved in Hepes buffer (pH = 7.4, 0.01 M) at the desired concentration, ε-PLL solution was in the basic form and it was converted to Cl salt by titration with HCl followed by extensive dialysis to eliminate H+ excess. Considering an apparent pKa of 7.5 for ε-PLL, it can be estimated that ~56% of the α-amino groups are protonated at physiological pH (~7.4).

Polymer decorating of LipoINH was obtained by adding polymer solutions, prepared at a proper concentration, to the liposome suspension, by considering mixing of equal volumes. After preparation, all samples were stored at 4 °C until their use in different experiments.

Table 1
Composition of the investigated samples: Lipo, INH-loaded liposomes (LipoINH) and polymer decorated liposomes (LipoINH + Chit and LipoINH + ε-PLL). Errors on concentration data are within 5%.

Sample	DPPG mg/mL	HSPC mg/mL	INH mg/mL	Chit mg/mL	ε-PLL mg/mL
Lipo	0.5	0.5	–	–	–
LipoINH	0.5	0.5	2.8	–	–
LipoINH + Chit	0.5	0.5	2.8	0.015	–
LipoINH + ε-PLL	0.5	0.5	2.8	–	0.015

2.3. Size, PDI, ζ-potential measurements

The hydrodynamic diameter (D_H), ζ-potential (ζ-pot), and polydispersity index (PDI) of all samples were characterized by Dynamic and Dielectrophoretic Light Scattering (DLS, DELS) using a Zetasizer Nano ZS90 instrument (Malvern Instruments, Worcestershire, UK), equipped with a 5 mW HeNe laser operating at a wavelength of 632.8 nm. Measurements were performed at a scattering angle of 90°, and the intensity autocorrelation function was analyzed using the Contin algorithm. The mean hydrodynamic radius and the polydispersity index (PDI) correspond to the intensity-weighted average, as typically done in similar analysis [35].

Electrophoretic mobility of the vesicles was assessed through laser Doppler velocimetry using the same instrument. The ζ-potential was derived from the measured mobility (μ) by applying the Smoluchowski equation: $\zeta = \mu\eta/\varepsilon$, where η denotes the solvent viscosity and ε its dielectric permittivity [36].

2.4. Determination of Isoniazid entrapment efficiency (EE%) and in vitro drug release studies

The entrapment efficiency (EE%) of INH in liposomal formulations was quantified by UV–visible spectrophotometry. Specifically, the amount of drug encapsulated within the liposomal vesicles was measured and compared to the initial amount of INH used during the preparation.

The EE% was calculated according to the following Eq. (1):

$$E.E.(\%) = \frac{Entrapped\ Isoniazid\ (mg)}{Total\ Isoniazid\ used\ (mg)} \times 100 \quad (1)$$

To ensure accurate absorbance measurements, samples were diluted in a solvent mixture consisting of Ethanol and Hepes buffer (70:30, v/v). The concentration of encapsulated INH was determined by measuring the absorbance at 263 nm using a UV–vis spectrophotometer (Lambda 25, PerkinElmer, Waltham, MA, USA).

In vitro drug release was investigated at 37 °C by placing 1 mL of sample (LipoINH, LipoINH + Chit, or LipoINH + ε-PLL) together with 1 mL of Hepes buffer (10 mM, pH 7.4) inside a dialysis tube. Alternatively, the Hepes buffer was replaced with cell culture medium (RPMI), simulated nasal fluid (SNF), or simulated lung fluid (SLF), depending on the experimental conditions. A cellulose acetate membrane (MWCO 8000, Spectra/Por®, diffusion area 5.5 cm^2) was used. The dialysis bag was then immersed in an external medium consisting of an ethanol:HEPES mixture (1:1, v/v) and maintained under continuous magnetic stirring. To determine the amount of INH released, aliquots of 1 mL were withdrawn from the release medium to perform UV analysis as described above, and then re-inserted back in the external medium. Analysis has been performed immediately after sampling, at different time points.

2.5. Fluorescence anisotropy

To evaluate the fluidity of liposomal bilayers, fluorescence anisotropy experiments were conducted using 1,6-diphenyl-1,3,5-hexatriene (DPH) as a fluorescent probe. Lipo, LipoINH, LipoINH + Chit and LipoINH + ε-PLL were investigated. DPH was added by co-dissolution with lipids in the organic mixture prior to film formation, at a final concentration of 2×10^{-4} M, following the protocol detailed in Section 2.2. Fluorescence measurements were carried out using a luminescence spectrometer (LS5013, PerkinElmer, Waltham, MA, USA). Excitation and emission wavelengths were set to 400 nm and 425 nm, respectively [33].

Fluorescence anisotropy (r), was calculated using the following Eq. (2):

$$r = \frac{(I_{VV} - GI_{VH})}{(I_{VV} + 2GI_{VH})} \quad (2)$$

where I_{VV}, I_{VH}, I_{HV}, and I_{HH} are the fluorescence intensities with vertical (V) or horizontal (H) orientations of excitation and emission polarizers. The G factor, defined as $G = I_{HV}/I_{HH}$, is the ratio of sensitivity of detection systems for vertically and horizontally polarized light.

2.6. Nebulization studies

Size distribution, PDI, ζ-potential, INH Entrapment Efficiency % and fluorescence anisotropy were also measured after nebulization by a jet nebulizer (Nebula Air Liquide Medical Systems S.p.A., Bovezzo, Italy), in order to evaluate the resistance of samples to this administration process, with the same procedure described in Forte et al. [37].

It is well known that liposomes can undergo physical instability during the nebulization process, leading to the disruption of the lipid bilayers, vesicle fragmentation, and significant loss of encapsulated hydrophilic molecules [19].

2.7. Morphological investigation (Transmission Electron Microscopy)

Particle morphology and shape of all liposomal samples pre and post-nebulization were investigated by transmission electron microscope. 40 μL of liposomal suspensions were placed on a strip of parafilm and Formvar/carbon-coated copper grids were allowed to swim on the surface of the droplets for 5 min. After adsorption, the grids were sequentially moved onto a series of Hepes buffer droplets for washing. The samples were then stained with 2% phosphotungstic acid (PTA) solution adjusted to pH 7.2, air-dried and examined under the electron microscope (Fei 208S, FEI Company, Hillsboro, OR, USA). Sample visualizations were performed by using a Mega-view II SIS camera (Olympus, Microscopy Technologies, Tokyo, Japan) at an accelerating voltage of 100 kV.

2.8. Preparation of mucin solution and mucoadhesive studies

Mucin powder was dissolved in Hepes buffer to prepare a 2 mg/mL solution at pH 6.0, which was then stirred continuously overnight at 34 °C. Key parameters such as temperature (34 °C), mucin concentration (2 mg/mL), and pH range (6.3–6.7) were carefully maintained during the mucoadhesive experiments to closely replicate the physiological environment of the lung. The mucin solution (2 mg/mL) was combined with liposome and polymer-decorated liposome suspensions in a 1:1 volume ratio, incubated at 34 °C [38] and subsequently analyzed using DLS and DELS.

2.9. Stability studies upon storage and in biological and simulated fluids

The stability of Lipo, Lipo INH, LipoINH + Chit, and LipoINH + ε-PLL formulations was evaluated over a period of 90 days at both 4 °C and room temperature. At predetermined time points (1, 30, 60, and 90 days), each sample was characterized by measuring particle size and ζ-potential using DLS and DELS.

Concurrently, stability studies of free INH and INH encapsulated within liposomes were performed under the same temperature conditions over the same time frame. These analyses were conducted using a Perkin-Elmer Lambda 25 UV–Vis double-beam spectrophotometer. The absorbance values of INH were recorded at a wavelength (λ) of 263 nm.

Stability assessments of the liposomal samples in the presence of cell culture medium (RPMI) were carried out. An aliquot of each sample was mixed in a test tube with an equal volume of RPMI medium and incubated at 37 °C in a water bath on a heating plate for 72 h. Samples were withdrawn hourly for the first 8 h, and subsequently at 24, 48 and 72 h. Each collected aliquot was analyzed by DLS to monitor potential changes in the hydrodynamic diameter of the liposomal systems.

In addition, sample stability studies were also conducted in Simulated Nasal Fluid (SNF) and in Simulated Lung Fluid (SLF) at 34 °C and 37 °C respectively, to assess the integrity and stability of the samples assuming their administration by inhalation.

SNF and SLF were prepared according to Trenkel et al. [39] and Marques et al. [40] respectively, and the composition is reported in Tables S1 and S2.

Mixtures of samples (50% v/v) and SNF or SLF (50% v/v) were prepared and incubated at their respective temperatures. Analyses were performed at different time intervals (0, 1, 2, and 3 h) by DLS to evaluate possible variations of particle size and the resistance of the formulations at these media.

2.10. Biological evaluation

2.10.1. Mycobacterial strain

Mycobacterium bovis BCG Pasteur strain, transformed with the plasmid carrying *Vibrio harveyi* luciferase gene, luxAB, in shuttle plasmid pSMT1 (BCG-lux), kindly provided by Prof. R. Reljic from St. George's University of London (UK), was used to evaluate intracellular mycobacterial viability, as described. BCG-lux was grown in Middlebrook 7H9 (Difco) broth supplemented with 10% ADC (albumin, dextrose and catalase), and 0.05% Tween 80, and titred by Colony Forming Unit (CFU) assay performed in Middlebrook 7H10 (Difco) supplemented with 10% OADC (oleic acid, albumin, dextrose and catalase) plates. To get ready-to-use titrated bacterial aliquots, grown BCG-lux was harvested, aliquoted in sterile PBS added with 10% glycerol and stored at −80 °C until use. To ensure plasmid maintenance, 50 μg/mL Hygromycin B (Invitrogen) was added in both 7H9 culture media and in 7H10 agar plates.

2.10.2. BCG-lux luminescence/CFU correlation

To validate the luminometric signal obtained from BCG-lux as an effective and reproducible indicator of mycobacterial viability, a correlation curve between BCG-lux relative luminescence units (RLU) and BCG-lux CFU was calculated. In detail, BCG-lux was grown in fully supplemented 7H9 broth; its growth was assessed via contextual luminometry (Fig. S1, Panel A) and CFU assay (Fig. S1, Panel B) at predetermined timepoints: T0, T1, T3, T6, T8, T13 (in days). For luminometric analysis, mycobacterial suspension and 1% decanal (as luciferase substrate) were resuspended in PBS at the ratio 1:1:8, respectively. Data are expressed as a Replication Index, calculated as the ratio between the mean Relative Luminescence Units (RLU) obtained at each timepoint and the mean RLU value obtained at T0. Luminescence was recorded by Varioskan LUX Multimode Microplate reader (Thermo Fisher Scientific). For CFU assay, a BCG-lux aliquot from each timepoint was serially diluted in PBS Tween80 0,05% and finally plated in triplicate on fully supplemented 7H10 plates. Finally, the interpolation between luminescence signals and CFU counts allowed the generation of a linear regression curve (Fig. S1, Panel C).

2.10.3. Cell line

Human promonocytic THP-1 leukemia cell line was supplied by the European Collection of Cell Culture, and were cultured as in Poerio et al. [41]. In particular, for the experiments, cells were seeded in 24-well plates at the concentration of 5×10^5/mL or in 96-well plates at the concentration of 1×10^6/mL for 72 h in the presence of 20 ng/mL Phorbol 12-Myristate 13-Acetate (Merck Life Science), getting differentiated THP-1 (dTHP-1).

2.10.4. Viability assay

dTHP-1 cells (2 × 105 per well) were stimulated with empty or INH-loaded liposomes decorated or not with either Chit or ε-PLL, or free INH. Both free INH and INH-loaded liposomes, regardless of their decoration, were accordingly diluted to achieve an INH concentration of its MIC value for BCG Pasteur strain: [0,1 μg/mL] [42], based on their INH EE%.

Finally, all empty liposomes were used identically as INH-loaded ones. After 72 h, cell viability was monitored by the MTT Cell Proliferation Assay Kit (Molecular Probe). Briefly, culture medium was removed and replaced with labelling culture medium (RPMI 1640 without phenol red, fully supplemented). The MTT assay is based on the cleavage of the yellow tetrazolium salt MTT (3-(4,5-Dimethylthiazol-2-yl)-2,5-diphenyltetrazolium bromide) to purple formazan crystals in metabolically active cells. Formazan is then solubilized using dimethyl sulfoxide (DMSO) 0.01 M, and the concentration determined by optical density at 540 nm. The assay is sensitive with the colorimetric signal proportional to the viable cell number. As negative control, all cell types were treated with 0.1% saponin at 37 °C for 30 min.

2.10.5. Evaluation of direct mycobactericidal effect

BCG-lux ($2{,}5 \times 10^6$ per well) were seeded in a 24-multiwell plate and stimulated for 72 h with empty or INH-loaded liposomes decorated or not with either Chit or ε-PLL, or free INH [0.1 μg/mL]. BCG-lux growth was monitored by luminometric assay, as previously described in Section 2.10.2, immediately after the stimulation and at day 3 post-treatment.

2.10.6. Evaluation of intracellular mycobactericidal effect

dTHP-1 cells were distributed in triplicate in 24 well plate (5×10^5 cells per well) and exposed for 3 h to BCG-lux at the multiplicity of infection (MOI) of 5. After removal of extracellular bacilli, cells were washed twice with PBS and finally cells were treated for 72 h with empty or INH-loaded liposomes decorated or not with either Chit or ε-PLL, or free INH. INH, where present, was used 0.1 μg/mL. After cell lysis via 30 mins incubation with 0.1% saponin, intracellular BCG-lux growth was monitored, as previously described in Section 2.10.2, by luminometric assay performed immediately after the infection and at day 3 post-infection.

2.11. Statistical analysis

The results are expressed as the means of three independent experiments ± standard deviation (S.D.). The data were evaluated for statistical significance using the student's *t*-test of Excel (Microsoft Office Professional Plus 2019) and one-way analysis of variance (ANOVA). Differences were considered statistically significant when $p < 0.05$. Significance levels are indicated as follows: $p \geq 0.05$: ns (not significant), $p < 0.05$: *, $p < 0.01$: **, $p < 0.001$: ***, $p < 0.0001$: ****.

Results of biological characterization are expressed as the mean of two or three independent experiments ± standard deviation. The statistical analysis of biological data was performed by using two-tailed Student's *t*-test.

3. Results and discussion

3.1.1. Physico-chemical and morphological characterization

HSPC–DPPG based liposomes were characterized by investigating their hydrodynamic diameter (D_H), ζ-Potential (ζ-Pot), polydispersity index (PDI), INH entrapment efficiency, anisotropy and pH values (Table 2).

Empty and INH-loaded liposomes exhibited hydrodynamic diameters of 218 nm and 231 nm, respectively, with a slight expansion due to osmotic pressure effect of the hydrophilic drug [43]. These values fall within the optimal size range (100–300 nm) for nasal administration and subsequent pulmonary delivery [44,45], where particle size is a critical parameter influencing deposition efficiency and transport through the nasal cavity.

The addition of the polymeric decoration (Chit and ε-PLL)was carried out with caution, so as not to significantly alter the physicochemical properties of the formulation. The appropriate concentration of Chit and ε-PLL has been selected on the basis of the "reentrant condensation" behavior of polymer-decorated liposomes, as shown in Fig. 1. The addition of Chit and ε-PLL on HSPC-DPPG liposomes promotes the formation of polymer-decorated particles with a hydrodynamic diameter progressively increasing up to a maximum, and ζ-potential approaching to zero, where aggregation of polymer-decorated particles occurs, then by further addition of polymer charge inversion and overcharging occur, and size decreases again. As extensively described in literature, this phenomenology is driven by the correlated adsorption of polyelectrolytes at the surface of oppositely charged particles [46,47]. This behavior shows that ζ-potential, size and stability can be tuned by choosing the appropriate amount of polymer. A small polycation content causes slight modifications and ensures the most appropriate condition for ensuring the suitable mucoadhesion, a good colloidal stability and an effective passage through the nasal environment.

Indeed, DLS analysis confirmed that the addition of these polymers, at low concentration, led only to a slight increase in hydrodynamic diameter compared to the LipoINH, without pushing the system outside the ideal size range.

As for the ζ-potential, a notable difference was observed between empty and INH-loaded liposomes (LipoINH in Table 2). While the empty liposomes exhibited a surface charge of approximately −41 mV, INH-loaded liposomes showed a significantly more negative value, around −51 mV. This shift suggests the modification of the surface of the INH-loaded liposomes connected to the adsorption of the drug at the lipid bilayer, as discussed in a previous investigation [33]. It has been found that INH, due to its dipolar nature at physiological pH, is able to interact with the zwitterionic lipid HSPC by dipole-dipole interaction and with the anionic polar head of DPPG via the positive region of its dipole. As a result, INH is not confined solely into the aqueous core, but it can adsorb and intercalate within the bilayer, exposing negatively charged functional groups at the liposome surface [48].

Following the addition of the polyelectrolytes, Chit and ε-PLL, a moderate reduction in surface charge was observed. The ζ-potential became less negative, measuring approximately −45 mV for LipoINH + Chit and − 44 mV for LipoINH + ε-PLL, compared to −51 mV for the LipoINH (Table 2). The slight reduction is consistent with the adsorption of polycations onto anionic liposomes [49], which partially neutralizes their negative charge at low polycation concentrations, in agreement with reentrant condensation (Fig. 1). This fine tuning was intentional: a shift toward positive surface charge could promote strong interactions with nasal mucus, leading to vesicle entrapment and clearance, thus hindering lung delivery. Therefore, maintaining a sufficiently negative ζ-potential is essential to ensure colloidal stability [50] and effective transport through the nasal environment [51].

Table 2
Physicochemical features of polymer-decorated liposomal formulations, as prepared (before aerosolization). Data of bare liposomes are reported as a reference. Errors are the standard deviations (SD) of data.

Sample	D_H ± SD (nm)	PDI ± SD	ζ-pot ± SD (mV)	[INH] ± SD (mg/mL)	E.E. % ± SD	Anisotropy ± SD	pH ± SD
Lipo	218 ± 2	0.18 ± 0.02	−41 ± 1	–	–	0.20 ± 0.01	7.4 ± 0.1
LipoINH	231 ± 2	0.20 ± 0.08	−51 ± 2	0.24 ± 0.02	8.5 ± 1.0	0.27 ± 0.01	7.4 ± 0.1
LipoINH + Chit	252 ± 5	0.25 ± 0.04	−45 ± 1	0.24 ± 0.02	8.5 ± 1.0	0.28 ± 0.02	5.9 ± 0.1
LipoINH + ε-PLL	253 ± 1	0.24 ± 0.07	−44 ± 2	0.24 ± 0.02	8.5 ± 1.0	0.26 ± 0.01	6.1 ± 0.1

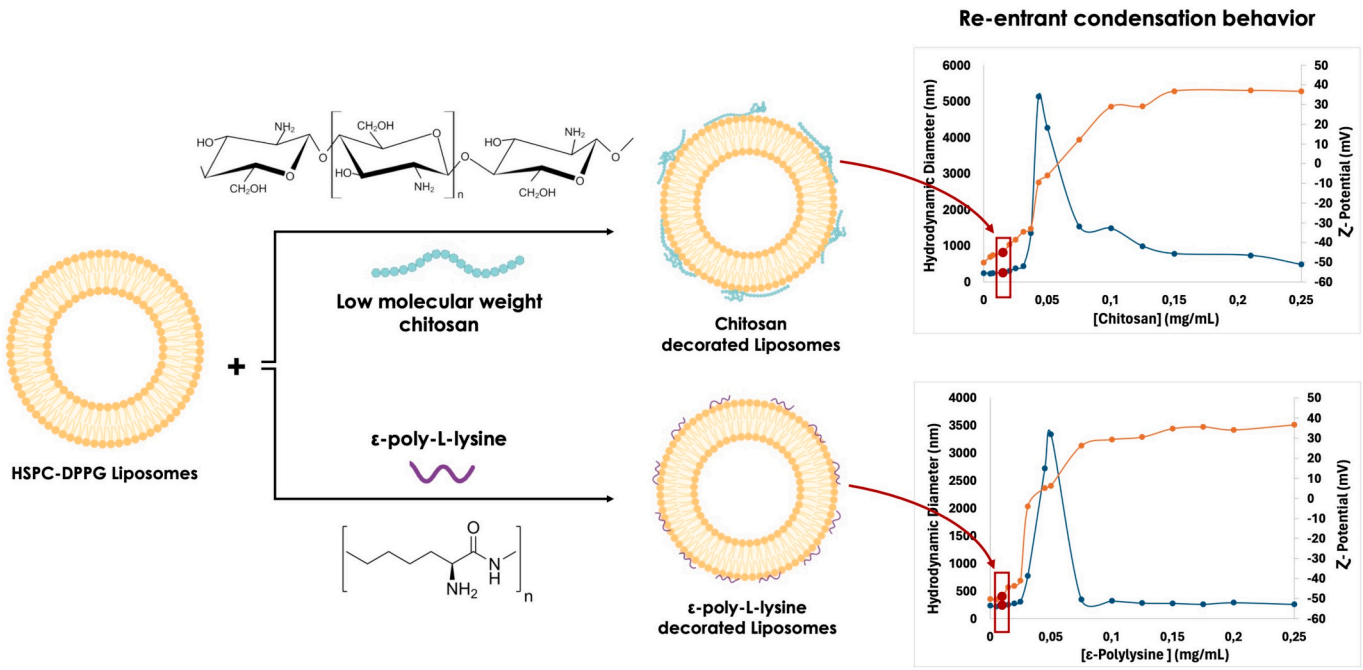

Fig. 1. Schematic representation of the formation of polymer-decorated HSPC-DPPG liposomes with Chitosan or ε-polylysine and their reentrant condensation behavior, with the gradual, non-monotonous increase of particle size in dependence of the polyelectrolyte concentration, associated with the progressive charge neutralization, charge inversion and overcharging of the polymer-decorated liposomes. At low polycation content a slight modification of size and ζ-potential of the polymer-decorated liposomes is observed: this condition can be identified as the most appropriate for ensuring the suitable mucoadhesion, a good colloidal stability and an effective passage through the nasal environment.

Additionally, the PDI values remained low for all samples, indicating the presence of a monodisperse population. Achieving a monodisperse system is essential for the correct interpretation of in vivo data, as homogeneous particles are more likely to follow similar biological pathways and exhibit consistent pharmacokinetic and biodistribution profiles. Indeed, the effectiveness of nanocarriers depends not only on their mean size but also on their PDI and physical stability [52].

As reported in Table 2, the pH values of the polymer-decorated formulations were 5.9 ± 0.1 and 6.1 ± 0.1 for Chit- and ε-PLL-decorated liposomes, respectively, remaining within the range generally considered compatible for nasal administration [53]. These pH conditions favor an increased fraction of protonated groups on the polyelectrolytes, thus guaranteeing a persistent positive surface charge that promotes strong electrostatic interactions with the negatively charged mucin network. In this context, particular attention was paid to evaluating how these two polycations with different chain flexibility and chemical structure of the repeating unit are able to adsorb on INH-loaded liposomes and how they affect the vesicular surface and overall organization (such as bilayer rigidity), as demonstrated in studies of INH-loaded liposomes, reporting the influence of drug–lipid interactions on bilayer packing, entrapment efficiency, and stability [33].

Finally, fluorescence anisotropy measurements provided further insight into the structural organization and dynamics of the liposomal bilayer. As reported in Table 2, the increase in anisotropy upon INH loading indicates a significant rigidification of the lipid bilayer, suggesting that the presence of the drug influences the internal structure of the membrane. This effect is connected to the strong drug-lipid interaction with a drug accumulation at the lipid bilayer and its eventual intercalation, as discussed in previous work [33]. Furthermore, the addition of Chit and ε-PLL did not produce further significant variations in anisotropy, which remained comparable to the values observed for INH-loaded liposomes. This suggests that the presence of these polyelectrolytes does not alter bilayer fluidity. Such behavior is consistent with their preferential localization at the liposomal surface, where they form a coating without penetrating the lipid bilayer or altering lipid-lipid organization and ordering or hydration.

As expected, based on the data discussed above, Chit and ε-PLL do not influence the EE% of INH, which remains constant at 0.24 mg/mL for all samples. This EE% is slightly higher than the reported values for Isoniazid found in Sciolla et al., who described E.E.% in the range of 1–2% for INH-loaded HSPC–DPPG liposomes with different formulation and lipid composition [33].

3.1.2. *Nebulization studies*

Nebulization was performed using the Nebula® aerosol therapy modulator system to simulate nasal aerosol delivery and evaluate formulation stability under mechanical stress. As reported in Table 3, no significant changes in the main physicochemical parameters were observed after nebulization for any of the formulations. In particular, only a slight decrease in hydrodynamic diameter was detected, while ζ-potential values remained essentially unchanged. Importantly, all size values remained within the optimal range for nasal-to-lung delivery, indicating that the aerosolization process did not induce aggregation or vesicle disruption.

TEM images (Fig. 2) evidenced the almost spherical shape for all samples, with a size comparable to the one determined by DLS measurements, both before and after nebulization. Samples observed after nebulization appeared intact and without ruptures or damages, with no significant dimensional changes or shape modifications, suggesting that the surface decoration performed with Chit and ε-PLL protect liposomes from structural changes.

3.2. *Stability studies upon storage and in biological and simulated fluids*

To evaluate the stability of decorated and undecorated LipoINH, all samples were stored at room temperature and at 4 °C for a period of 60 days. As shown in Fig. 3 Panels A, C, E, the size of all samples (LipoINH, LipoINH + Chit and LipoINH + ε-PLL) increase over time when stored at room temperature. This trend may be attributed to vesicle aggregation or fusion processes, likely promoted by enhanced molecular mobility

Table 3
Physicochemical features of polymer-decorated liposomal formulations, after nebulization process. Data of bare liposomes are reported as a reference. Errors are the standard deviations (SD) of data.

Sample (post nebulization)	$D_H \pm$ SD (nm)	PDI ± SD	ζ-pot ± SD (mV)	[INH] ± SD (mg/mL)	E.E. % ± SD	Anisotropy ± SD	pH ± SD
Lipo	204 ± 2	0.25 ± 0.02	−30 ± 1	–	–	0.22 ± 0.01	7.4 ± 0.1
LipoINH	215 ± 5	0.28 ± 0.08	−51 ± 2	0.22 ± 0.01	8.2 ± 1.0	0.29 ± 0.01	7.4 ± 0.1
LipoINH + Chit	230 ± 6	0.35 ± 0.02	−47 ± 1	0.23 ± 0.02	8.3 ± 1.0	0.29 ± 0.02	5.9 ± 0.1
LipoINH + ε-PLL	223 ± 4	0.32 ± 0.04	−45 ± 2	0.22 ± 0.01	8.2 ± 1.0	0.27 ± 0.01	6.1 ± 0.1

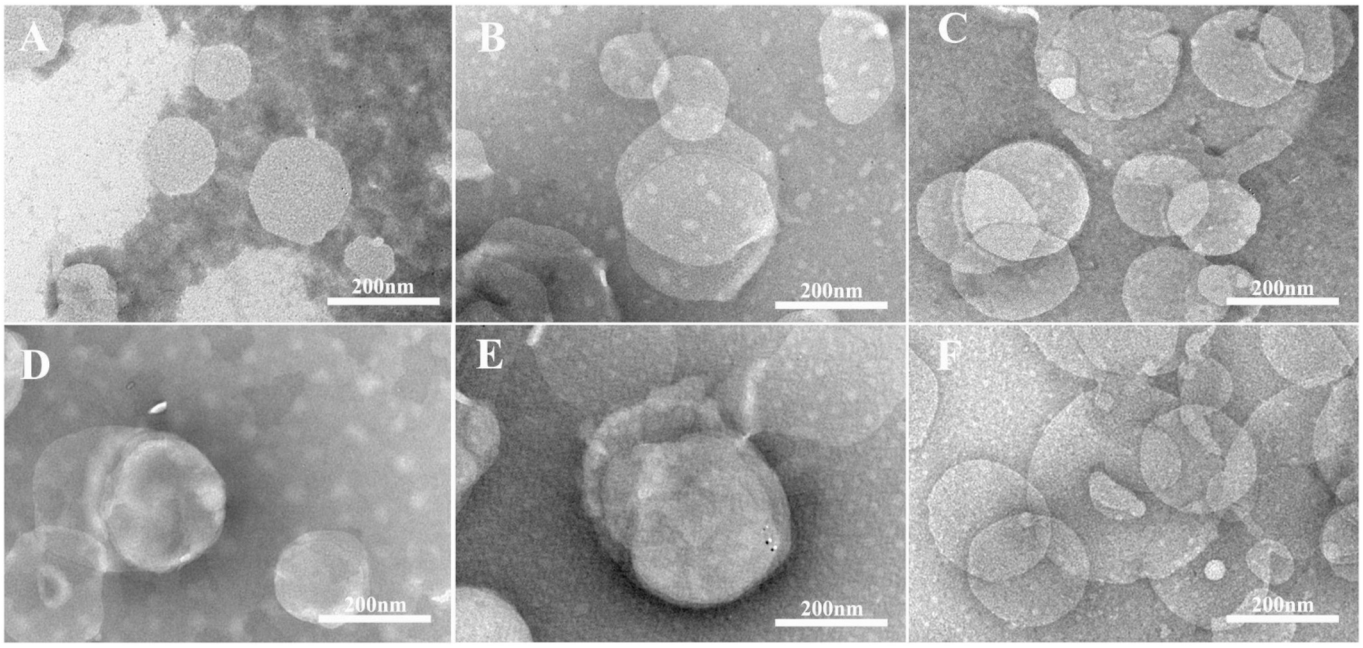

Fig. 2. TEM micrographs of liposomal formulations (negative staining) before (A, B, and C) and after (D, E, and F) nebulization. LipoINH (A and D), LipoINH + Chit (B and E,) and LipoINH + ε-PLL (C and F).

and decreased membrane stability at higher temperatures. In contrast, storage at 4 °C (Fig. 3, Panels B, D, F) can maintain the particle size within the same range as the initial measurements, guaranteeing the necessary colloidal stability for the formulations. Fig. 4 demonstrates a difference in the stability profile of free INH versus its liposomal form. Specifically, UV-spectrum of free INH is characterized by a decrease in absorbance values over the 90-day storage period at both tested temperatures (data not shown), resulting in the determination of a lower amount of drug, as reported in Fig. 4, Panel A, while INH in liposomes tend to maintain greater stability under the same conditions (Fig. 4, Panel B). The presence of the Chit or ε-PLL decoration does not alter the stability profile of INH when encapsulated in liposomes, as expected for a surface decorating which does not interfere with the structure of an INH-loaded liposome. Importantly, the presence of the Chit or ε-PLL decoration does not appear to affect the stability of INH within the liposomes, as would be expected for a surface decorating that primarily interacts with the liposome exterior rather than the encapsulated drug. We can conclude that in most experimental conditions, both for Chit and ε-PLL-based formulations, INH appears more stable when encapsulated in liposomes and polymer decorated-liposomes, compared to the free drug especially at 4 °C. These findings suggest that liposomal inclusion may provide a stabilizing effect, supporting its potential utility in enhancing the stability of the active pharmaceutical ingredient.

At the outset of our stability assessment, the stability of empty and loaded liposomes, decorated and undecorated, was evaluated in RPMI culture medium (Fig. 5, Panel A), which is the same medium employed in bioactivity assays, and the experiment was carried out at the same conditions (time and temperature).

Notably, after contact with RPMI, it is possible to observe an increase in particle size of decorated samples with respect to undecorated ones. Probably, the polyelectrolytes on the liposomal surface interact with the various components of RPMI medium, particularly proteins and other macromolecules. The size increase does not suggest system breakdown.

In contrast, when the formulations were in contact with simulated nasal and lung fluids (SNF and SLF), no significant changes in particle size were observed (Fig. 5, Panels B and C), indicating a high colloidal stability of both decorated and undecorated liposomes in these simulated media. This behavior can be attributed to the simpler composition of SNF and SLF, which lack the high concentration of proteins and macromolecules present in RPMI.

From a functional standpoint, the lack of size increase in SNF and SLF represents a favorable outcome, as it indicates minimal nonspecific interactions between the liposomal surface and surrounding fluid components. This aspect is particularly relevant for nasal and pulmonary delivery, where preservation of the nanocarrier's original surface properties may promote more selective interactions with the mucus layer and target epithelium, rather than being obscured by the formation of a biomolecular corona. Overall, these findings further support the suitability of the proposed liposomal systems for administration in nasal and pulmonary environments.

3.3. *Mucoadhesion studies*

The ability to interact with mucin represents a key feature for in vivo efficacy of the nanocarriers designed for lung delivery. For this purpose, we carried out an investigation to obtain information on the interaction

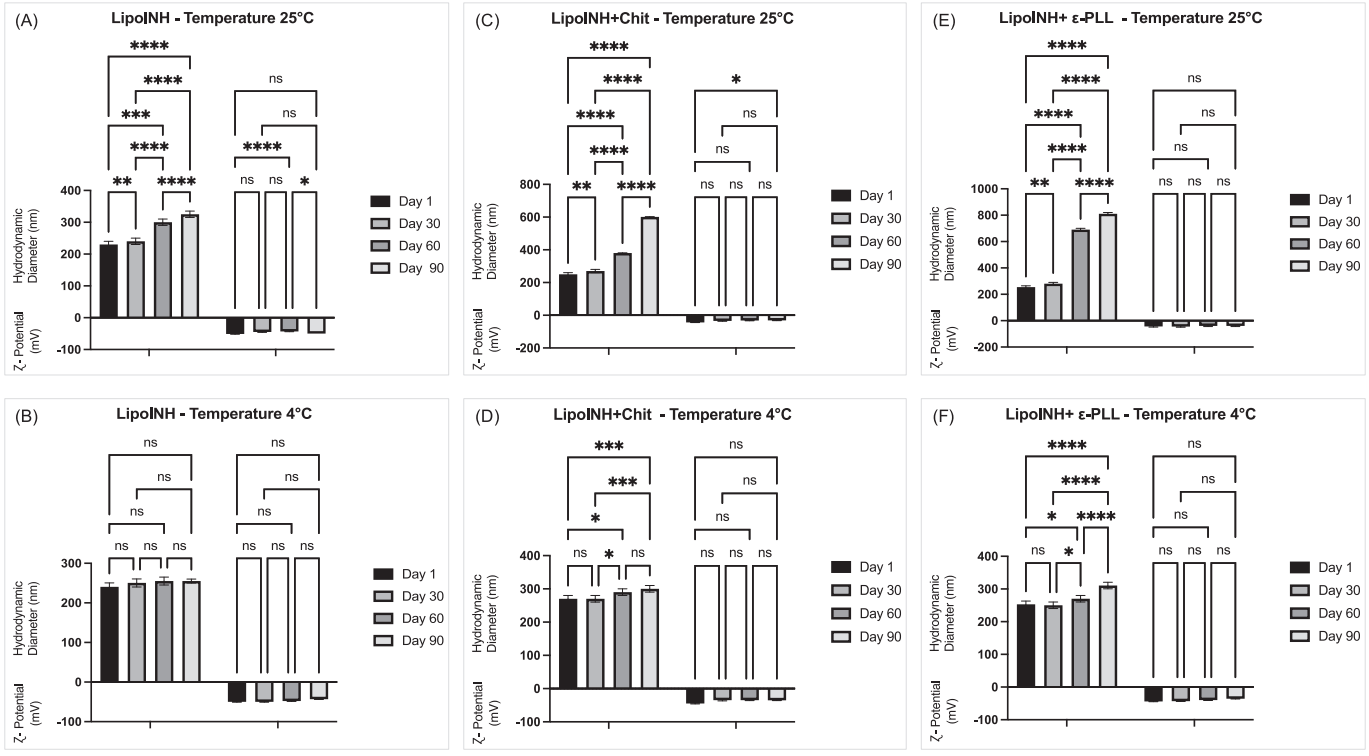

Fig. 3. Result of investigation on physicochemical stability of liposomes until up to 90 days at room temperature and 4 °C. Data were obtained as the average of three independent experiments. ns $p \geq 0.05$, * $p < 0.05$, ** $p < 0.01$, *** $p < 0.001$, **** $p < 0.0001$.

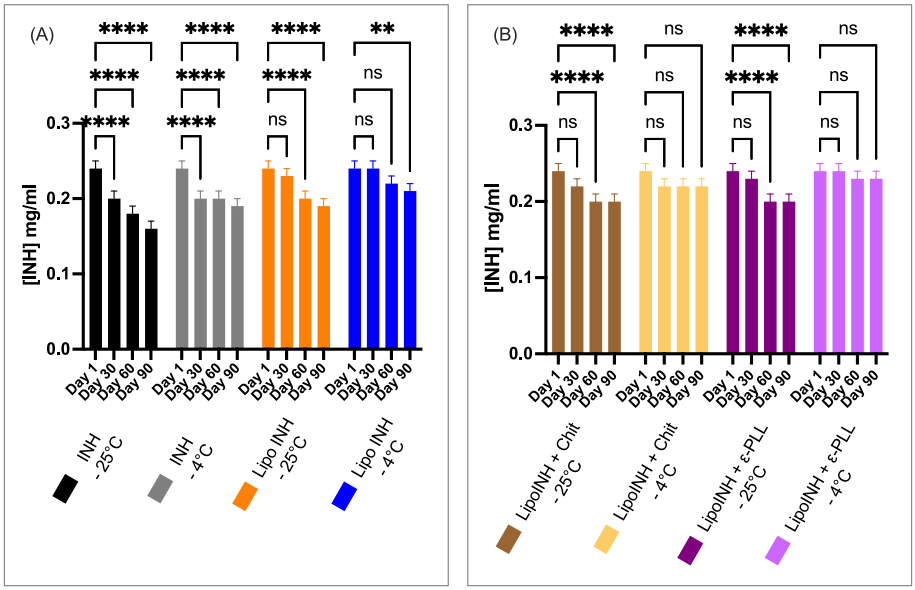

Fig. 4. Stability studies over time of free INH (Panel A) and INH-loaded liposomes (Panel B) at 2 different storage temperatures over a 90-day period. Data were obtained as the average of three independent experiments. ns p ≥ 0.05, * p < 0.05, ** p < 0.01, *** p < 0.001, **** p < 0.0001.

between polymer-decorated liposomes and mucin by measuring the hydrodynamic diameter of the samples. Obtained results are reported in Fig. 6. After mucin addition, a significant increase in size was observed for the polymer-decorated sample compared with undecorated liposomes. No significant difference is observed for Chit and ε-PLL decorated-liposomes. This finding suggests that the ε-PLL-decorating can confer liposomes the same mucoadhesive property of the most frequently used Chit polymer.

3.4. Release studies

Fig. 7, Panel A shows the release profiles of INH from LipoINH, LipoINH + Chit, and LipoINH + ε-PLL. The amount of INH released from the liposomes was comparable regardless of polymer decoration, demonstrating that the optimized surface coating preserves the intrinsic properties and release profile of the nanocarriers. It is important to highlight that the same release profile was also observed in the presence of the culture medium and simulated fluids, as shown in Fig. 7, Panels B,

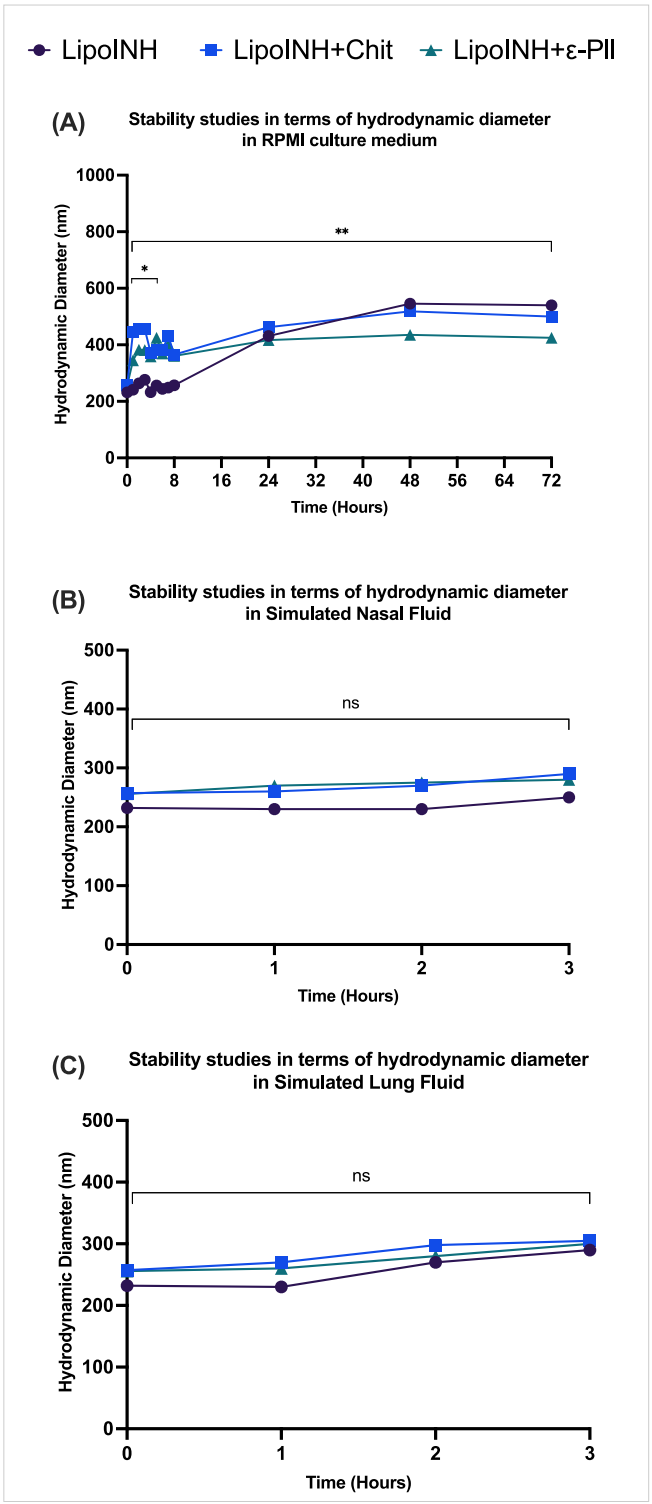

Fig. 5. Effect of RPMI culture media (Panel A), Simulated Nasal Fluid (Panel B) and Simulated Lung Fluid (Panel C) on hydrodynamic diameter of samples at different incubation times. Data were obtained as the average of three independent experiments. ns $p \geq 0.05$, * $p < 0.05$, ** $p < 0.01$, *** $p < 0.001$, **** $p < 0.0001$.

C, D.

Fig. S2 shows the release profiles of INH until up to 72 h, to mimic in vitro biological experiments.

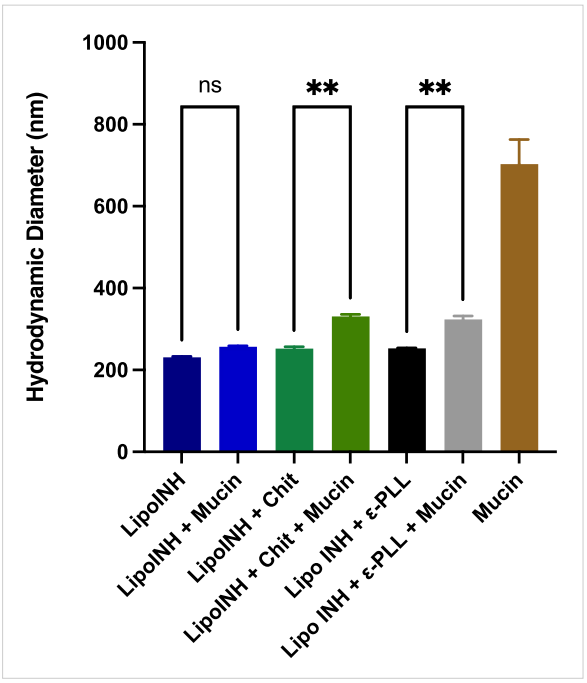

Fig. 6. Interaction between samples and mucin investigated by measuring hydrodynamic diameter. Data were obtained as the average of three independent experiments. ns $p \geq 0.05$, * $p < 0.05$, ** $p < 0.01$, *** $p < 0.001$, **** $p < 0.0001$.

3.5. Biological evaluation

Developing new strategies against *Mycobacterium tuberculosis* is challenging due to its slow growth and strict biosafety requirements. In this context, the recombinant BCG-lux strain, emitting light proportional to bacterial viability (Fig. S1), enabled rapid monitoring of infection [54]. On these grounds, BCG-lux–infected macrophages were treated with free INH, INH-loaded and unloaded liposomes, either undecorated or functionalized with Chit or ε- PLL, in order to evaluate intracellular bacterial viability after 3 days. As shown in Fig. 8A, both free INH and INH-loaded liposomes significantly reduced intracellular mycobacterial viability, with a more significant effect for encapsulated INH, irrespective of surface decoration. Notably, unloaded liposomes had no measurable impact on either intracellular or extracellular bacterial survival (Figs. 8A and S3), confirming that the antibacterial activity was exclusively due to INH.

Furthermore, the release profile (Fig. S2) showed an antibiotic leakage plateau of approximately 50% after 3 days, supporting liposome stability in culture and indicating that antibiotic delivery primarily occurred through liposomes intracellular uptake. Finally, macrophage viability assessed by MTT assay (Fig. 8B) showed no significant differences between treated and untreated cells, confirming the absence of the possible INH cytotoxicity [55] and supporting the safety profile of such liposome formulations.

4. Conclusion

The present study demonstrates the feasibility of developing inhalable mucoadhesive liposomal nanocarriers through a simple and mild strategy based on polymer decoration. By exploiting electrostatic interactions between INH-loaded anionic liposomes and cationic polyelectrolytes, it was possible to modulate surface properties while preserving the intrinsic structural and physicochemical features of the carrier, including size, bilayer organization, drug entrapment efficiency, colloidal stability and release behavior. A key outcome of this work is the comparative evaluation of two polycations with well distinct

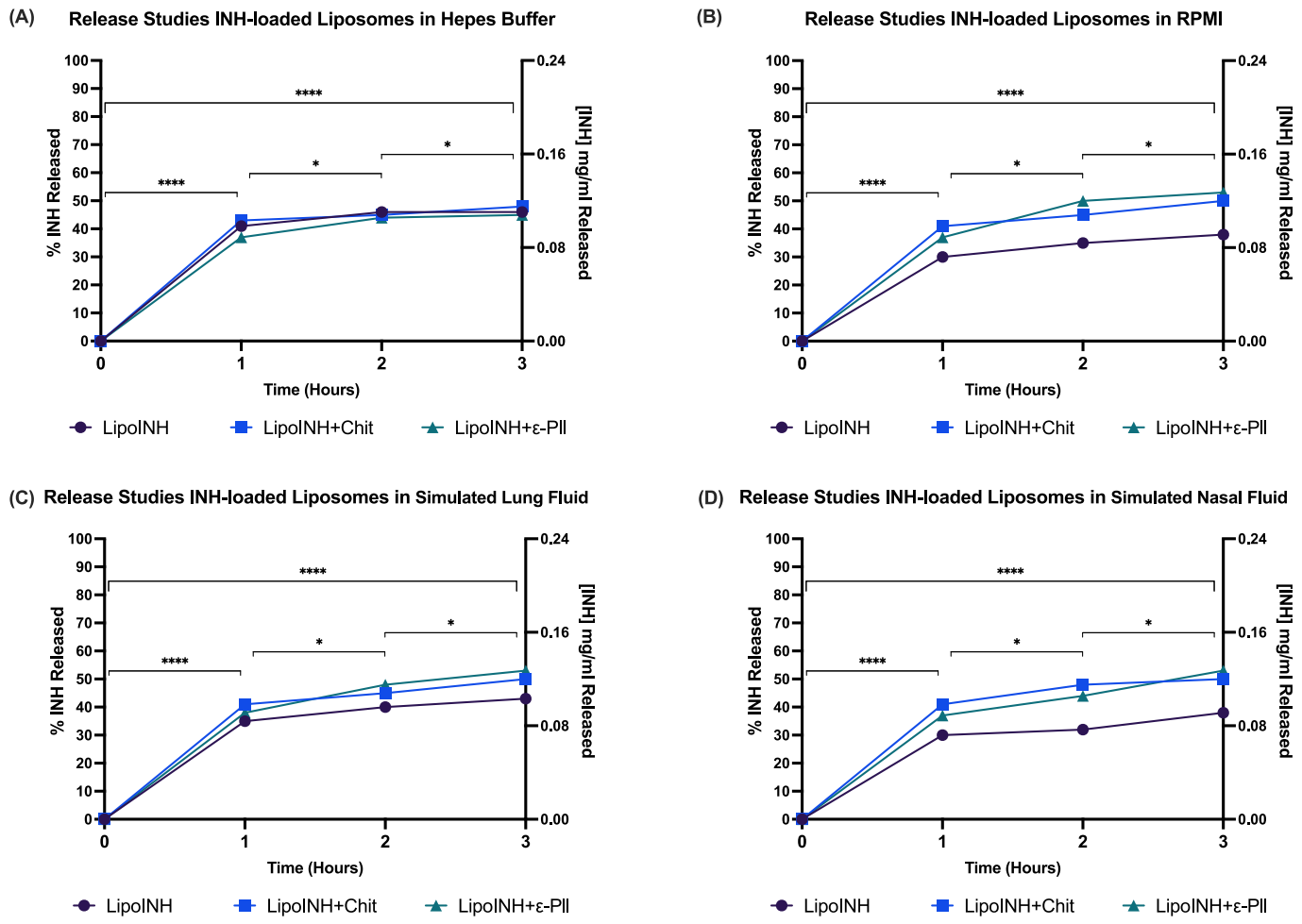

Fig. 7. INH release profile until up to 3 h in Hepes Buffer (Panel A), in RPMI culture media (Panel B), in Simulated Nasal Fluid (Panel C) and in Simulated Lung Fluid (Panel D). Data were obtained as the average of three independent experiments. ns $p \geq 0.05$, * $p < 0.05$, ** $p < 0.01$, *** $p < 0.001$, **** $p < 0.0001$.

macromolecular characteristics, chitosan and ε-poly-L-lysine (ε-PLL). While chitosan is widely recognized as a benchmark mucoadhesive polymer, our results show that also ε-PLL-decorated liposomes exhibit physicochemical stability, mucoadhesive behavior, aerosolization resistance, and intracellular delivery efficacy fully comparable to those of chitosan-decorated systems. Moreover, ε-PLL decoration, similarly to chitosan, does not alter liposome integrity, bilayer fluidity, or drug release kinetics, confirming its surface-localized interaction and the presence of electrostatic adsorption without destabilizing effects.

The stability of the polymer-decorated liposomal formulations under conditions relevant to nasal and pulmonary administration, including nebulization and exposure to simulated biological fluids, further supports their suitability for nose-to-lung delivery. In addition, the enhanced intracellular antibacterial efficacy observed for INH-loaded liposomes, compared to free drug, highlights the potential of this platform for targeting intracellular mycobacterial infections, without inducing cytotoxic effects on host cells. Overall, these findings identify the still scarcely explored ε-PLL as a promising natural biocompatible polymer for liposomal surface functionalization. Compared to chitosan, ε-PLL offers an alternative, supporting both safety and therapeutic efficacy. To the best of our knowledge, this is the first investigation describing the use of ε-PLL to improve specific nanocarriers features, such as mucoadhesion, drug delivery efficiency and cell internalization, of liposomal formulations. The simplicity, versatility, and effectiveness of this approach may open new perspectives for the rational design of inhalable nanocarriers and encourage further investigations into ε-PLL-based surface modifications for advanced drug delivery applications.

CRediT authorship contribution statement

Jacopo Forte: Writing – review & editing, Writing – original draft, Validation, Methodology, Investigation, Data curation, Conceptualization. **Tommaso Olimpieri:** Visualization, Validation, Methodology, Investigation, Data curation. **Noemi Poerio:** Writing – review & editing, Writing – original draft, Visualization, Validation, Supervision, Methodology, Investigation, Data curation, Conceptualization. **Leonardo Severini:** Visualization, Validation, Data curation. **Maurizio Fraziano:** Writing – review & editing, Supervision, Conceptualization. **Maria Grazia Ammendolia:** Writing – review & editing, Visualization, Validation, Data curation. **Federica Rinaldi:** Writing – review & editing, Writing – original draft, Supervision, Methodology, Investigation, Conceptualization. **Simona Sennato:** Writing – review & editing, Writing – original draft, Investigation, Funding acquisition, Conceptualization. **Carlotta Marianecci:** Writing – review & editing, Supervision, Conceptualization. **Federico Bordi:** Writing – review & editing, Supervision, Funding acquisition, Conceptualization. **Maria Carafa:** Writing – review & editing, Supervision, Funding acquisition, Conceptualization.

Ethical statement

The study was conducted in compliance with the current ethical guidelines of the Italian authority and according to the Declaration of Helsinki Principles.

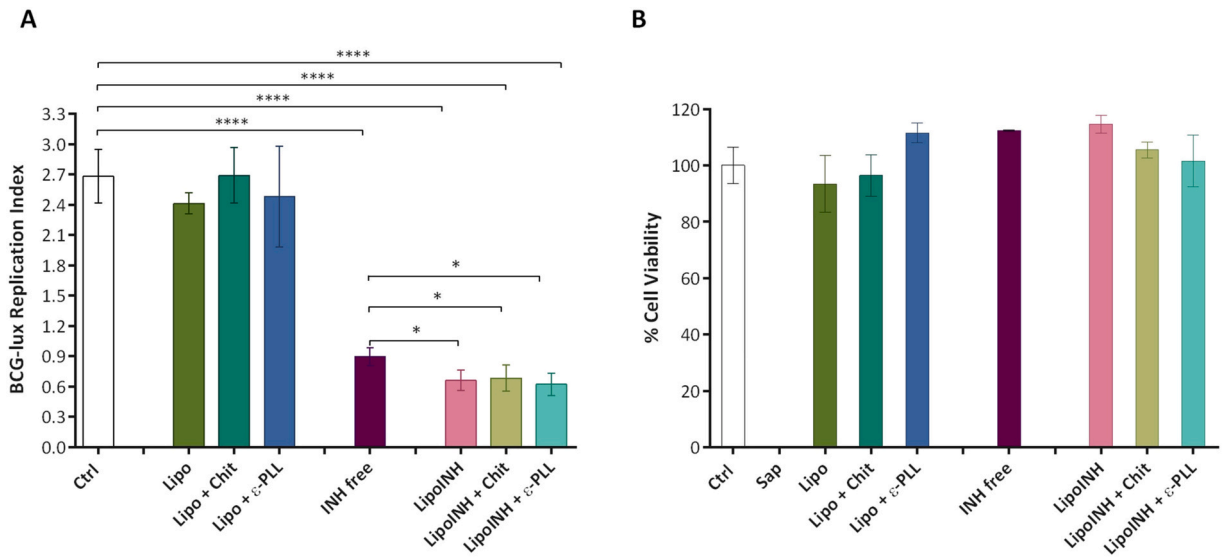

Fig. 8. Intracellular mycobacterial killing is improved by INH-loaded liposomes with no cytotoxicity effect. (A) dTHP-1 (5×10^5 cells/mL) were infected with BCG-lux (MOI 5) for 3 h, then extracellular bacilli were removed by washing cells twice with PBS and finally they were treated with empty or INH-loaded liposomes decorated or not with either Chit or ϵ-PLL, or free INH. Both free INH and INH-loaded liposomes, regardless of their decoration, were accordingly diluted to achieve an Isoniazid concentration of 0,1 μg/mL. Mycobacterial growth was evaluated by luminometric analysis immediately after infection (T0) and at 3 days from stimulation (T3). Data are shown as means ± SD of the ratio T3/T0 of RLU values from triplicate cultures and are representative of at least 2 independent experiments. Statistical analysis was performed by using two-sided Student's *t*-test. *$p < 0.05$, ****$p < 0.0001$. If not indicated by the line, the comparisons were performed versus control. (B) dTHP-1 (2 × 105 cells/200 μL) were stimulated with empty or INH-loaded liposomes decorated or not with either Chit or ϵ-PLL, or free INH for 72 h and then were subjected to MTT Assay. Both free INH and INH-loaded liposomes, regardless of their decoration, were accordingly diluted to achieve an Isoniazid concentration of 0,1 μg/mL. As negative control, cells were treated with 0.1% saponin (Sap) at 37 °C for 30 min. Results are shown as mean ± standard deviation (SD) of OD540nm values performed in triplicate and are representative of two independent experiments.

Funding

S. S. acknowledge Lipoid for the kind gift of lipids and financial support under the National Recovery and Resilience Plan (NRRP), Mission 4, Component 2, Investment 1.3, Call for tender No. 341 published on 15.3.2022 by the Italian Ministry of University and Research (MUR), funded by the European Union - NextGenerationEU – Project "One Health Basic and Translational Research Actions addressing Unmet Needs on Emerging Infectious Diseases—INFACTPE00000007"– CUP B53C20040570005. S.S., F. B. and M.C. acknowledge financial support from Phospholipid Research Center (Grant n. FBO-2017-051/1-1). T.O. was supported by PNRR project ESC00000024 – Rome Technopole.

Declaration of competing interest

The authors declare that they have no known competing financial interests or personal relationships that could have appeared to influence the work reported in this paper.

Appendix A. Supplementary data

Supplementary data to this article can be found online at https://doi.org/10.1016/j.ijbiomac.2026.152914.

Data availability

Data will be made available on request.

References

[1] C. Sebaaly, A. Trifan, E. Sieniawska, H. Greige-Gerges, Chitosan-coating effect on the characteristics of liposomes: a focus on bioactive compounds and essential oils: a review, Processes 9 (2021) 445, https://doi.org/10.3390/pr9030445.
[2] S. Chen, S. Huang, Y. Li, C. Zhou, Recent advances in epsilon-poly-L-lysine and L-lysine-based dendrimer synthesis, modification, and biomedical applications, Front. Chem. 9 (2021), https://doi.org/10.3389/fchem.2021.659304.
[3] M. Bassetti, A. Vena, A. Russo, M. Peghin, Inhaled liposomal antimicrobial delivery in lung infections, Drugs 80 (2020) 1309–1318, https://doi.org/10.1007/s40265-020-01359-z.
[4] W. Lin, R. Goldberg, J. Klein, Poly-phosphocholination of liposomes leads to highly-extended retention time in mice joints, J. Mater. Chem. B 10 (2022) 2820–2827, https://doi.org/10.1039/D1TB02346B.
[5] Y. Cao, X. Dong, X. Chen, Polymer-modified liposomes for drug delivery: from fundamentals to applications, Pharmaceutics 14 (2022) 778, https://doi.org/10.3390/pharmaceutics14040778.
[6] H. Yadav, R. Malviya, N. Kaushik, Chitosan in biomedicine: a comprehensive review of recent developments, Carbohydr. Polym. Technol. Appl. 8 (2024) 100551, https://doi.org/10.1016/j.carpta.2024.100551.
[7] H. Honarkar, M. Barikani, Applications of biopolymers I: chitosan, Monatsh. Chem. 140 (2009) 1403–1420, https://doi.org/10.1007/s00706-009-0197-4.
[8] C. Thambiliyagodage, M. Jayanetti, A. Mendis, G. Ekanayake, H. Liyanaarachchi, S. Vigneswaran, Recent advances in chitosan-based applications—a review, Materials 16 (2023) 2073, https://doi.org/10.3390/ma16052073.
[9] S. Kumar, J. Dutta, P.K. Dutta, J. Koh, A systematic study on chitosan-liposome based systems for biomedical applications, Int. J. Biol. Macromol. 160 (2020) 470–481, https://doi.org/10.1016/j.ijbiomac.2020.05.192.
[10] J.M. Joy, A. P, R.J. M, P.K. Dara, V. Renuka, R. Anandan, Liposome mediated encapsulation and role of chitosan on modulating liposomal stability to deliver potential bioactives-a review, Food Hydrocoll. Health 4 (2023) 100142, https://doi.org/10.1016/j.fhfh.2023.100142.
[11] I. Singh, S. Kumar, S. Singh, M.Y. Wani, Overcoming resistance: chitosan-modified liposomes as targeted drug carriers in the fight against multidrug resistant bacteria-a review, Int. J. Biol. Macromol. 278 (2024) 135022, https://doi.org/10.1016/j.ijbiomac.2024.135022.
[12] Y. Liu, D. Liu, L. Zhu, Q. Gan, X. Le, Temperature-dependent structure stability and in vitro release of chitosan-coated curcumin liposome, Food Res. Int. 74 (2015) 97–105, https://doi.org/10.1016/j.foodres.2015.04.024.
[13] F. Zhou, T. Xu, Y. Zhao, H. Song, L. Zhang, X. Wu, B. Lu, Chitosan-coated liposomes as delivery systems for improving the stability and oral bioavailability of acteoside, Food Hydrocoll. 83 (2018) 17–24, https://doi.org/10.1016/j.foodhyd.2018.04.040.
[14] C.-M. Lehr, J.A. Bouwstra, E.H. Schacht, H.E. Junginger, In vitro evaluation of mucoadhesive properties of chitosan and some other natural polymers, Int. J. Pharm. 78 (1992) 43–48, https://doi.org/10.1016/0378-5173(92)90353-4.
[15] P.L. Devine, I.F.C. McKenzie, Mucins: structure, function, and associations with malignancy, BioEssays 14 (1992) 619–625, https://doi.org/10.1002/bies.950140909.
[16] S.K. Lai, Y.-Y. Wang, J. Hanes, Mucus-penetrating nanoparticles for drug and gene delivery to mucosal tissues, Adv. Drug Deliv. Rev. 61 (2009) 158–171, https://doi.org/10.1016/j.addr.2008.11.002.

[17] C. Marianecci, L.D. Marzio, F. Rinaldi, M. Carafa, F. Alhaique, Pulmonary delivery: innovative approaches and perspectives, JBNB 02 (2011) 567–575, https://doi.org/10.4236/jbnb.2011.225068.
[18] M.H. Elkomy, A.A. Ali, H.M. Eid, Chitosan on the surface of nanoparticles for enhanced drug delivery: a comprehensive review, J. Control. Release 351 (2022) 923–940, https://doi.org/10.1016/j.jconrel.2022.10.005.
[19] J. Forte, P.N. Hanieh, N. Poerio, T. Olimpieri, M.G. Ammendolia, M. Fraziano, M. G. Fabiano, C. Marianecci, M. Carafa, F. Bordi, S. Sennato, F. Rinaldi, Mucoadhesive rifampicin-liposomes for the treatment of pulmonary infection by Mycobacterium abscessus: chitosan or ε-poly-L-lysine decoration, Biomolecules 13 (2023) 924, https://doi.org/10.3390/biom13060924.
[20] F. Rinaldi, P.N. Hanieh, S. Sennato, F. De Santis, J. Forte, M. Fraziano, S. Casciardi, C. Marianecci, F. Bordi, M. Carafa, Rifampicin–liposomes for *Mycobacterium abscessus* infection treatment: intracellular uptake and antibacterial activity evaluation, Pharmaceutics 13 (2021) 1070, https://doi.org/10.3390/pharmaceutics13071070.
[21] T. Yoshida, T. Nagasawa, ε-Poly-l-lysine: microbial production, biodegradation and application potential, Appl. Microbiol. Biotechnol. 62 (2003) 21–26, https://doi.org/10.1007/s00253-003-1312-9.
[22] B. Rodrigues, T.P. Morais, P.A. Zaini, C.S. Campos, H.O. Almeida-Souza, A. M. Dandekar, R. Nascimento, L.R. Goulart, Antimicrobial activity of epsilon-poly-l-lysine against phytopathogenic bacteria, Sci. Rep. 10 (2020) 11324, https://doi.org/10.1038/s41598-020-68262-1.
[23] E. Lebaudy, C. Guilbaud-Chéreau, B. Frisch, N.E. Vrana, P. Lavalle, The high potential of ε-poly-l-lysine for the development of antimicrobial biomaterials, Adv. NanoBiomed Res. 3 (2023) 2300080, https://doi.org/10.1002/anbr.202300080.
[24] A. Alemán, I. Mastrogiacomo, M.E. López-Caballero, B. Ferrari, M.P. Montero, M. C. Gómez-Guillén, A novel functional wrapping design by complexation of ε-polylysine with liposomes entrapping bioactive peptides, Food Bioproc. Tech. 9 (2016) 1113–1124, https://doi.org/10.1007/s11947-016-1703-4.
[25] M. Li, Y. Tao, Poly (ε-lysine) and its derivatives via ring-opening polymerization of biorenewable cyclic lysine, Polym. Chem. 12 (2021) 1415–1424.
[26] A.E. Gad, B.L. Silver, G.D. Eytan, Polycation-induced fusion of negatively-charged vesicles, Biochim. Biophys. Acta Biomembr. 690 (1982) 124–132, https://doi.org/10.1016/0005-2736(82)90246-2.
[27] S. Rao, M. Sun, Y. Hu, X. Zheng, Z. Yang, X. Jiao, ε-Polylysine-coated liposomes loaded with a β-CD inclusion complex loaded with carvacrol: Preparation, characterization, and antibacterial activities, LWT 146 (2021) 111422, https://doi.org/10.1016/j.lwt.2021.111422.
[28] S. Sennato, F. Bordi, C. Cametti, C. Marianecci, M. Carafa, M. Cametti, Hybrid niosome complexation in the presence of oppositely charged polyions, J. Phys. Chem. B 112 (2008) 3720–3727, https://doi.org/10.1021/jp0775449.
[29] C. Agrati, C. Marianecci, S. Sennato, M. Carafa, V. Bordoni, E. Cimini, M. Tempestilli, L.P. Pucillo, F. Turchi, F. Martini, G. Borioni, F. Bordi, Multicompartment vectors as novel drug delivery systems: selective activation of Tγδ lymphocytes after zoledronic acid delivery, Nanomed. Nanotechnol. Biol. Med. 7 (2011) 153–161, https://doi.org/10.1016/j.nano.2010.10.003.
[30] K. Shi, Y. Liu, L. Ke, Y. Fang, R. Yang, F. Cui, Epsilon-poly-l-lysine guided improving pulmonary delivery of supramolecular self-assembled insulin nanospheres, Int. J. Biol. Macromol. 72 (2015) 1441–1450, https://doi.org/10.1016/j.ijbiomac.2014.10.023.
[31] C.I. Nkanga, R.W.M. Krause, Encapsulation of isoniazid-conjugated phthalocyanine-in-cyclodextrin-in-liposomes using heating method, Sci. Rep. 9 (2019) 11485, https://doi.org/10.1038/s41598-019-47991-y.
[32] M. Altaf, C.H. Miller, D.S. Bellows, R. O'Toole, Evaluation of the *Mycobacterium smegmatis* and BCG models for the discovery of *Mycobacterium tuberculosis* inhibitors, Tuberculosis 90 (2010) 333–337, https://doi.org/10.1016/j.tube.2010.09.002.
[33] F. Sciolla, D. Truzzolillo, E. Chauveau, S. Trabalzini, L. Di Marzio, M. Carafa, C. Marianecci, A. Sarra, F. Bordi, S. Sennato, Influence of drug/lipid interaction on the entrapment efficiency of isoniazid in liposomes for antitubercular therapy: a multi-faced investigation, Colloids Surf. B Biointerfaces 208 (2021) 112054, https://doi.org/10.1016/j.colsurfb.2021.112054.
[34] L. Severini, L. Tavagnacco, S. Sennato, E. Celi, E. Chiessi, C. Mazzuca, E. Zaccarelli, Unveiling the self-assembly process of gellan-chitosan complexes through a combination of atomistic simulations and experiments, Int. J. Biol. Macromol. 292 (2025) 139098, https://doi.org/10.1016/j.ijbiomac.2024.139098.
[35] A. Imbriano, F. García-Villén, J. Forte, M. Ruggeri, A. Lasalvia, F. Rinaldi, L. Perioli, G. Sandri, C. Marianecci, C. Viseras, M. Carafa, Clay-carvacrol nanoemulsions for wound healing: Design and characterization studies, J. Drug Delivery Sci. Technol. 99 (2024) 105984, https://doi.org/10.1016/j.jddst.2024.105984.
[36] I.M. Tucker, J.C.W. Corbett, J. Fatkin, R.O. Jack, M. Kaszuba, B. MacCreath, F. McNeil-Watson, Laser Doppler electrophoresis applied to colloids and surfaces, Curr. Opin. Colloid Interface Sci. 20 (2015) 215–226, https://doi.org/10.1016/j.cocis.2015.07.001.
[37] J. Forte, E. D'Intino, F. Cappiello, C. Vetrano, M.G. Fabiano, A. Viscido, M. G. Ammendolia, B. Casciaro, F. Rinaldi, M. Carafa, M.L. Mangoni, C. Marianecci, Optimization of aerosolizable and bioactive essential oils-based nanoemulsions: Physico-chemical and biological characterization, Colloids Surf. B Biointerfaces 253 (2025) 114733, https://doi.org/10.1016/j.colsurfb.2025.114733.
[38] R.C. Boucher, Airway surface dehydration in cystic fibrosis: pathogenesis and therapy, Annu. Rev. Med. 58 (2007) 157–170, https://doi.org/10.1146/annurev.med.58.071905.105316.
[39] M. Trenkel, R. Scherließ, Nasal powder formulations: in-vitro characterisation of the impact of powders on nasal residence time and sensory effects, Pharmaceutics 13 (2021) 385, https://doi.org/10.3390/pharmaceutics13030385.
[40] M.R.C. Marques, R. Loebenberg, M. Almukainzi, Simulated biological fluids with possible application in dissolution testing, Dissolut. Technol. 18 (2011) 15–28, https://doi.org/10.14227/DT180311P15.
[41] N. Poerio, N.R. Caccamo, M.P. La Manna, T. Olimpieri, L.H. De Angelis, M. M. D'Andrea, F. Dieli, M. Fraziano, Phosphatidylserine liposomes reduce inflammatory response, mycobacterial viability, and HIV replication in coinfected human macrophages, J. Infect. Dis. 225 (2022) 1675–1679, https://doi.org/10.1093/infdis/jiab602.
[42] N. Ritz, M. Tebruegge, T.G. Connell, A. Sievers, R. Robins-Browne, N. Curtis, Susceptibility of *Mycobacterium bovis* BCG vaccine strains to antituberculous antibiotics, Antimicrob. Agents Chemother. 53 (2009) 316–318, https://doi.org/10.1128/AAC.01302-08.
[43] T. Kure, H. Sakai, Transmembrane difference in colloid osmotic pressure affects the lipid membrane fluidity of liposomes encapsulating a concentrated protein solution, Langmuir 33 (2017) 1533–1540, https://doi.org/10.1021/acs.langmuir.6b04643.
[44] C. Dhand, M.P. Prabhakaran, R.W. Beuerman, R. Lakshminarayanan, N. Dwivedi, S. Ramakrishna, Role of size of drug delivery carriers for pulmonary and intravenous administration with emphasis on cancer therapeutics and lung-targeted drug delivery, RSC Adv. 4 (2014) 32673–32689, https://doi.org/10.1039/C4RA02861A.
[45] M. Gagliardi, S. Chiarugi, C. De Cesari, G. Di Gregorio, A. Diodati, L. Baroncelli, M. Cecchini, I. Tonazzini, Crosslinked chitosan nanoparticles with muco-adhesive potential for intranasal delivery applications, IJMS 24 (2023) 6590, https://doi.org/10.3390/ijms24076590.
[46] S. Sennato, L. Carlini, D. Truzzolillo, F. Bordi, Salt-induced reentrant stability of polyion-decorated particles with tunable surface charge density, Colloids Surf. B Biointerfaces 137 (2016) 109–120, https://doi.org/10.1016/j.colsurfb.2015.06.011.
[47] F. Bordi, S. Sennato, D. Truzzolillo, Polyelectrolyte-induced aggregation of liposomes: a new cluster phase with interesting applications, J. Phys. Condens. Matter 21 (2009) 203102, https://doi.org/10.1088/0953-8984/21/20/203102.
[48] A.V. Marques, P. Marengo Trindade, S. Marques, T. Brum, E. Harte, M. O. Rodrigues, M.G.M. D'Oca, P.A. da Silva, A.R. Pohlmann, I.D. Alves, V.R. de Lima, Isoniazid interaction with phosphatidylcholine-based membranes, J. Mol. Struct. 1051 (2013) 237–243, https://doi.org/10.1016/j.molstruc.2013.08.029.
[49] D. Volodkin, H. Mohwald, J.-C. Voegel, V. Ball, Coating of negatively charged liposomes by polylysine: Drug release study, J. Control. Release 117 (2007) 111–120, https://doi.org/10.1016/j.jconrel.2006.10.021.
[50] R.H. Müller, C. Jacobs, O. Kayser, Nanosuspensions as particulate drug formulations in therapy: Rationale for development and what we can expect for the future, Adv. Drug Deliv. Rev. 47 (2001) 3–19, https://doi.org/10.1016/S0169-409X(00)00118-6.
[51] J.L. Antunes, J. Amado, F. Veiga, A.C. Paiva-Santos, P.C. Pires, Nanosystems, drug molecule functionalization and intranasal delivery: an update on the most promising strategies for increasing the therapeutic efficacy of antidepressant and anxiolytic drugs, Pharmaceutics 15 (2023) 998, https://doi.org/10.3390/pharmaceutics15030998.
[52] P.N. Hanieh, S. Consalvi, J. Forte, G. Cabiddu, A. De Logu, G. Poce, F. Rinaldi, M. Biava, M. Carafa, C. Marianecci, Nano-based drug delivery systems of potent MmpL3 inhibitors for tuberculosis treatment, Pharmaceutics 14 (2022) 610, https://doi.org/10.3390/pharmaceutics14030610.
[53] W. Kamin, A. Schwabe, I. Krämer, Physicochemical compatibility of fluticasone-17-propionate nebulizer suspension with ipratropium and albuterol nebulizer solutions, Int. J. Chron. Obstruct. Pulmon. Dis. 2 (2007) 599–607, https://doi.org/10.2147/copd.s12159995.
[54] M.J. Hickey, T.M. Arain, R.M. Shawar, D.J. Humble, M.H. Langhorne, J. N. Morgenroth, C.K. Stover, Luciferase in vivo expression technology: use of recombinant mycobacterial reporter strains to evaluate antimycobacterial activity in mice, Antimicrob. Agents Chemother. 40 (1996) 400–407, https://doi.org/10.1128/AAC.40.2.400.
[55] A.K. Verma, A. Yadav, S.V. Singh, P. Mishra, S.K. Rath, Corrigendum to "Isoniazid induces apoptosis: role of oxidative stress and inhibition of nuclear translocation of nuclear factor (erythroid-derived 2)-like 2 (Nrf2)" [Life Sci 119 (2018) 23-33], Life Sci. 240 (2020) 117136, https://doi.org/10.1016/j.lfs.2019.117136.